Numerical Methods in Civil Engineering, 9-3 (2025) 75-91

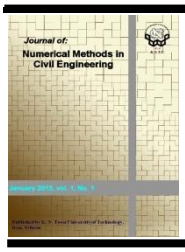

Numerical Methods in Civil Engineering

Journal Homepage: https://nmce.kntu.ac.ir/

Numerical modeling of new Ductile concrete material as infill wall

Tiam Shirzadi*

ARTICLE INFO

RESEARCH PAPER

Article history:
Received:
December 2024
Revised:
December 2024
Accepted:
February 2025

Keywords:
Infill wall,
RC frame,
DLFC,
FEM analyze,
Cyclic load,
NTHA curves

Abstract:

In urban construction, the prevalent use of reinforced concrete (RC) with masonry infill is challenged by the brittle nature of traditional masonry, which significantly increases seismic vulnerabilities. This research introduces a novel solution: Ductile Lightweight Fiber-Reinforced Concrete (DLFC) as an infill material. DLFC is composed of cement, water, expanded polystyrene (EPS), ultra-fine fillers, and a blend of polyvinyl alcohol (PVA) and polypropylene (PPF) fibers. The primary goal of using DLFC is to enhance ductility, reduce damage during seismic events, and improve energy absorption capabilities. One of the most important concerns of engineers is how to model the walls and their effects on the structure. In this study, the method of modeling the experimental element was discussed first, and then its effects on the structure were discussed with numerical modeling in the form of finite element and macro model. The analysis performed is a non-linear time history analysis, which was compared according to the bare and infill frame with DLFC blocks in SAC structures. The results show a decrease in the displacement of the roof of the structure and non-sensational shift of period in structure

1. Introduction

Reinforced concrete (RC) frames are the focus of much attention in seismic performance due to the potential for catastrophic destruction under seismic loading, which is not surprising given the substantial horizontal displacements they experience during acceleration. While the design of RC frames typically focuses on structural members, non-structural elements like masonry infill are often overlooked [1-3]. However, the presence of infill walls alters the overall structural behavior of RC frames. Specifically, they affect how the frames respond to lateral loads such as wind and seismic forces, contribute to the lateral stiffness of RC frames, reduce their deflection, and enhance their ability to withstand lateral loads [4, 5].

Additionally, the interaction between infill walls and the surrounding frame structure gives rise to intricate phenomena, including soft-story behavior, out-of-plane instability, and stress concentration [6-11]. These complexities have the potential to undermine the overall strength and flexibility of the structure. Hence, it seems crucial to conduct a comprehensive examination of how infill walls impact the rigidity, strength, and seismic performance of reinforced concrete frames. This investigation is essential for optimizing their design, guaranteeing structural integrity under diverse loading scenarios, and formulating effective retrofitting approaches that enhance their ability to withstand seismic activity [12]. Yet, in conventional practices of structural design, the main focus is primarily on the weight of the filling material, assuming that only the reinforced concrete elements are capable of withstanding lateral forces. Thus, the potential negative impacts of the infill are often disregarded. To address this issue, multiple studies have sought to examine and predict failure modes associated with the interaction between the infill and the frame members [6, 13]. Furthermore, the strength and construction of the infill components play a significant role in determining the specific failure mode. Therefore, it is essential to consider the influence of infill during the modeling process to ensure that the designed model accurately represents the behavior of the actual structure. Moreover, accurately capturing the intricate behavior of infill requires complex calculations rather than merely representing it as a compression strut or a shell element [14-18]. It is also important to note that the aforementioned interaction between infill materials and

* *Corresponding Author: Ph.D., Faculty of Civil Engineering, K.N. Toosi University of Technology, Tehran, Iran. Email: t.shirzadi@email.kntu.ac.ir*

https://doi.org/10.61186/NMCE.2412.1080

structural members must not be ignored, as it leads to an increase in shear within the stories [19]. Extensive research has been conducted to gain a deeper understanding of the impact of infill on structures and to minimize its influence over seismic behavior, owing to the difficulties posed by these challenges [20-29].

Different types of infill panel walls are used in construction, depending on factors like building design, materials, and functional requirements. Nonetheless, a promising option called ductile lightweight fiber has shown potential in improving the seismic behavior of RC frames. This material is renowned for its remarkable tensile strength and ductility. As a result, incorporating ductile lightweight fiber-reinforced concrete (DLFC) as an infill material offers exciting possibilities for enhancing the seismic performance of structures, particularly in areas with high seismic hazards. Its unique properties render it a compelling substitute for traditional masonry infill walls. The current study aimed to enhance several aspects related to the performance of RC frames using prefabricated DLFC blocks. The research involved conducting tests on the in-plane behavior of these frames, considering varying height-to-span ratios in three dimensions. The study compared several factors, including energy dissipation, damage propagation, lateral stiffness, damping ratio, seismic parameters, and out-of-plane behavior of the samples. The findings indicated that incorporating these infill walls in regions prone to powerful earthquakes can significantly enhance the structural behavior and minimize the extent of damage when compared to conventional frames. Regarding the primary focus of this study, firstly, it aimed to determine the seismic parameters of DLFC blocks with varying dimensions. It also contributed by providing valuable insights into the analysis of the failure modes and crack propagation that occur during the cyclic loading of the frame. Furthermore, the research cought to develop a mathematical formula that could be used to estimate the lateral strength of the infill wall. To effectively discuss the concept of infill walls in construction, it's essential to emphasize the structural gap that exists between the frame, columns, and beams. This gap, typically measuring around 0.01 times the height of the column, is crucial for accommodating insulation materials, such as rock wool, which enhance thermal performance. Furthermore, to prevent excessive out-of-plane displacement and ensure structural integrity, the installation of rabbits small reinforcing elements is employed. This method not only supports the overall stability of the structure but also contributes to its resilience against lateral forces.

Experimental studies have demonstrated that the incorporation of shear keys, which connect the beams and columns, significantly enhances the shear strength of infilled frames. These shear keys are strategically positioned within AAC (Autoclaved Aerated Concrete) blocks and are tailored to the dimensions of the wall. Their implementation has proven to be particularly effective in managing the out-of-plane behavior of the wall, thereby improving overall structural performance and stability.

2. Experimental Study

The experiments were conducted at a structural laboratory situated at K. N. Toosi University of Technology. This specific laboratory was furnished with advanced apparatus that could accurately replicate earthquakes by applying both vertical and horizontal forces simultaneously. The testing process comprised two main stages. Initially, the DLFC and mortar were subjected to various tests to ascertain their physical characteristics, with the findings subsequently documented in [30]. Moving on to the second stage, the focus shifted towards examining the RC frame materials, as well as subjecting the RC frames with DLFC infill to cyclic testing.

2.1 Specimen design

Three individual, single-span, single-story reinforced concrete moment frames were designed following the guidelines of the Iranian Seismic Design Code (Standard 2800). These frames were labeled as frames S1, S2, and S3 with respective height-to-span ratios of 1.28, 1, and 0.77. The dimensions of the beams and columns for all three frames were 250×250 mm. Longitudinal rebars with a diameter of 12 mm were utilized to reinforce both the beams and columns. Additionally, 10 mm diameter stirrups were placed at intervals of 75 mm within the beams and columns, and at intervals of 150 mm in the foundation. The angle of the stirrup hook was set at 135° for both the beams and columns. Additionally, the hook-free length was determined to be equivalent to 10 times the diameter of the stirrup. The columns were supported by a concrete foundation measuring 300×400, featuring longitudinal rebars with a diameter of 14 mm and 10 mm diameter stirrups, all detailed in Figure 1. It should be noted that all measurements of the specimens are in centimeters, as shown in the Figure. Furthermore, 14 mm diameter threaded bolts with a 90° bend were employed in the concrete foundation, and their positioning and construction specifications are depicted in Figure 1.

2.2 Specimen construction

2.2.1 Concrete frame

The process of constructing the RC frames is illustrated in Figure 2. In the beginning, molds made of wood were crafted for the specimens in a workshop specializing in MDF, and the steel reinforcement grids were positioned within them. These molds were elevated 5 cm above the ground with the help of wooden supports, making it convenient to lift the molds once the concrete had solidified. To ensure the correct

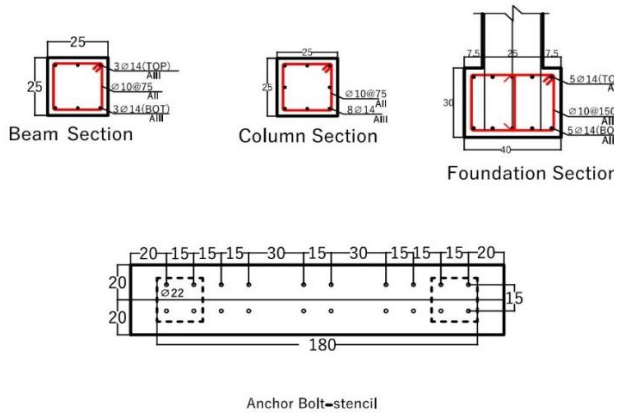

Fig. 1: Dimension and details of specimens

formation of the concrete cover, 5-cm spacers were inserted into the molds before laying down the rebar. The interior of the wooden molds underwent a thorough cleaning process using compressed air. Moreover, all concrete mold joints were carefully sealed with silicon glue to prevent any formation of joints in the concrete during its placement. The foundation mold's underside contained 20 bolt holes for securing it to the sturdy laboratory floor. A template was employed to guarantee the accurate alignment of the bolt holes on the mold with the holes on the solid floor. Subsequently, any potential errors or discrepancies that may arise during the process were minimized or eliminated. The positions of the holes on the solid floor were replicated onto the blueprint and then transferred onto the foundation mold. The mold underwent the final step of the creation process with the use of a laser cutting machine in the MDF workshop to produce the necessary holes.

To prevent any expansion during the concrete setting, the wooden forms were secured with iron wire. Then, the concrete was poured into the mold and consistently sprinkled with water, resulting in proper curing. After a 28-day duration dedicated to the process of setting and curing, the moment frames were elevated through the utilization of a crane and firmly affixed to the base with bolts that possess exceptional strength.

To minimize the potential for damage during handling the concrete frames were lifted using broad straps. This approach ensured that the risk of harm to the frames was significantly reduced, as the wide straps provided ample support for the heavy structures. By employing this method, the likelihood of any detrimental effects caused by mishandling or improper lifting techniques was significantly decreased. The use of wide straps proved to be an effective solution in safeguarding the integrity and structural stability of the concrete frames throughout the handling process [32]. The dimensions of the samples are equivalent to a 1/2 scale of the actual frame. It is noteworthy that samples S1, S2, and S3 were meticulously designed, taking into account various critical factors. These include the selection of materials, the applied loading system, the percentage of cross-sectional reinforcement, and all relevant design considerations for the frame. This thorough approach ensures that the scaled models effectively represent the structural behavior of full-scale frames.

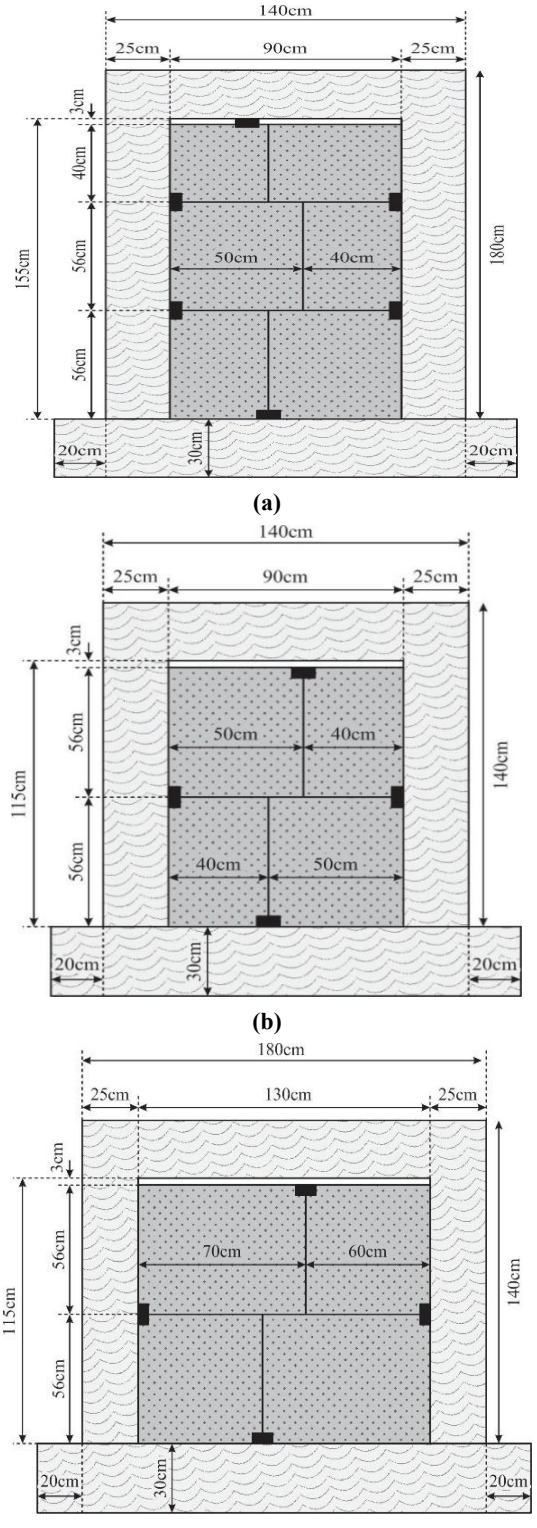

Fig. 2: Panels dimension (a) Sample S1, (b) Sample S2 and (c) Sample S3

2.2.2 DLFC Infill

The reinforced concrete frame incorporated DLFC infill panels, which were manufactured in the concrete workshop. These panels, characterized by their low shear strength, could be manually cut into custom dimensions using a cutting machine. Additionally, their connection interface featured male-female configurations to facilitate secure attachment. The panels' other surfaces were flat and were coated with mortar. To install the panels, U-shaped iron components with cross-sectional dimensions of 10×5×5 and a length of 10 mm were affixed to the beam and column at the panel joint locations using four nails. Subsequently, cementitious mortar, 10 mm in thickness, was utilized to secure the panels in place. Figure 2 provides details regarding the specifications, size, and placement of the panels, which had a consistent height of 56 cm and varied widths of 40 cm, 50 cm, 60 cm, and 70 cm, tailored to the frame dimensions. Notably, the panels could be easily resized as necessary. For ease of construction, a 3 cm-wide separation joint was incorporated between the panel and the upper beam. Due to their lightweight nature, the DLFC blocks were easily transportable. While the panels maintained a constant height of 56 cm, their widths were adjusted to suit the frames. Furthermore, they were arranged with a 10 cm joint width to enhance integrated performance during testing.

2.3 Material properties

2.3.1 DLFC Material

As depicted in Figure3, the DLFC composition comprised cement, water, ultra-fine filler, pumice, polystyrene, polypropylene fibers (PPF), polyvinyl alcohol fibers (PVA), and an emulsifier serving as a stabilizer. The DLFC formulation utilized 1% PVA and 1.5% PPF, with the physical properties of these. To produce the DLFC panels, the components illustrated in Figure 5 were initially blended, followed by molding and setting of the DLFC, and subsequently placement in curing chambers to facilitate water evaporation. After 28 days, the molds were opened, and the prefabricated panels were ready for use as infill walls. The DLFC materials were prepared by initially mixing the dry materials, such as cement and pumice, for 1.5 minutes, incorporating water, emulsions, and fibers, and further mixing for 5 minutes. Molds were customizable to various sizes, with the specimens used for testing possessing dimensions of 120×60×10 cm, featuring male-female connections as depicted in Figure 3. To assess the compressive strength of the DLFC samples, three specimens measuring 10×10×10 cm underwent compression tests, the results of which are presented in Figure 3.

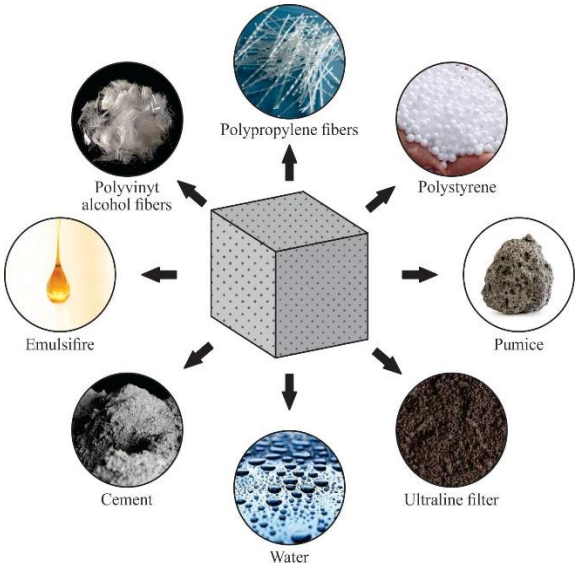

Fig. 3: Materials of lightweight concrete

2.3.2 Concrete and Steel Rebars

The concrete's compressive strength within the frame was assessed by testing 8 cubic specimens measuring 150×150cm. This evaluation yielded an average compressive strength of 30 MPa for the concrete. The steel employed for the longitudinal rebars in the beams, columns, and foundation bolts belonged to the A-III category with a yield strength (fy) of 400 MPa, while the steel utilized for the stirrups was categorized as A-II with a yield strength of 300 MPa. Tensile tests were conducted on the rebars using a universal testing machine, and the average test results are detailed in [32].

2.4 Test setup and loading protocol

The concrete frames were securely fastened to a rigid plate using 20 anchor bolts. To apply the horizontal load, a 500-kN hydraulic jack was employed. This jack was affixed to the vertical base using 30 friction bolts, and its end was fixed to the beam end using 8 anchor bolts and a 250 × 250 mm metal plate featuring 8 holes with a diameter of 17 mm, enabling the application of a cyclic load. Additionally, a 300-kN vertical jack was utilized to simulate the vertical load acting on the frame. The structure supporting the vertical jack was a truss designed to withstand and distribute vertical loads. Initially, the vertical jack was positioned on a load cell and a wide-flange steel beam (W-beam). Two rollers, made of steel with a diameter of 60 mm and a length of 250 mm, were employed on the rigid plates of the two columns and the W-beam to distribute the load between the columns. These rollers were fully coated in grease to facilitate smooth movement of the frame with minimal friction. The plates used on the columns had dimensions of 300×250×15 mm. The specifics of the test setup are illustrated in Figure 4.

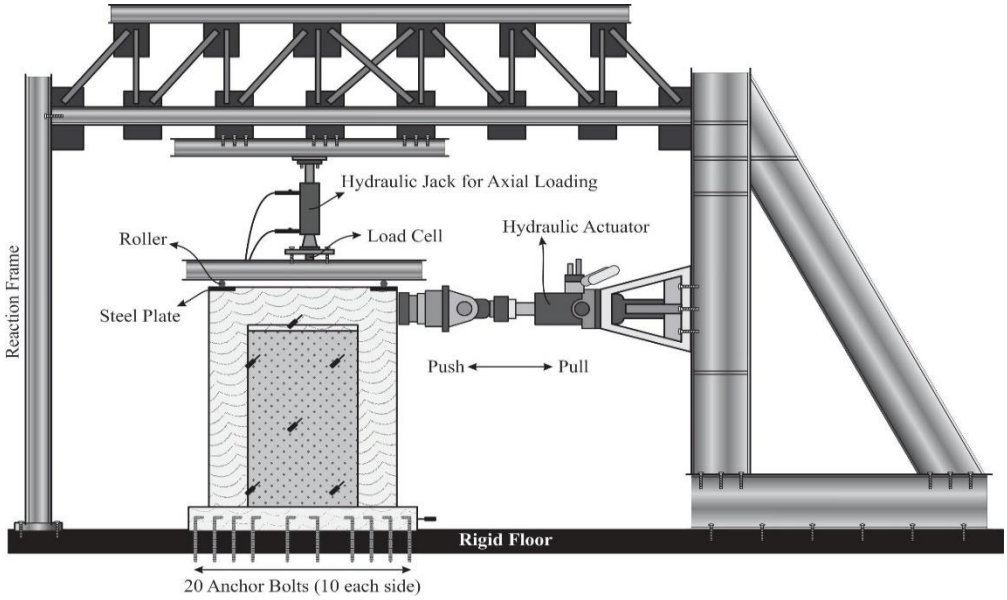

Fig. 4: Test setup

The reinforced concrete (RC) frames were simultaneously subjected to lateral and vertical loading. An axial load equivalent to approximately 15% of the columns' capacity was applied in the form of force control. Previous studies have utilized various loading protocols such as ATC-20, ISO 16670, and FEMA 461 [33] for lateral loading, all of which have yielded similar responses due to their comparable energy dissipation requirements. In this study, the FEMA 461 protocol [33] was employed due to its reasonable displacement steps. The loading steps of this protocol result in smaller and medium drifts, reducing the number of drifts at larger displacements. Moreover, this protocol allows for adjustments to time steps based on load cycles and in response to potential temperature increases in the hydraulic jack.

The mentioned quasi-static loading was applied in tension and compression, with the loading pattern taking the form of displacement control. The load was incrementally increased until reaching a final displacement of 119.5 cm. The tests were terminated when the ultimate strength decreased to approximately 85% of the maximum strength or when severe damage was observed in the specimens. Figure 8 illustrates the loading protocol.

2.5 Experimental results

The hysteresis diagrams of three samples are shown in Figure 5. These graphs have been measured in different time steps. As shown, the slope of the graphs is initially upward, and then due to the non-linearity of the materials, the slope of the graphs decreased. Backbone curves were obtained for numerical simulations and obtaining seismic parameters. In this curve, the maximum values of the hysteresis curve are connected to create this curve.

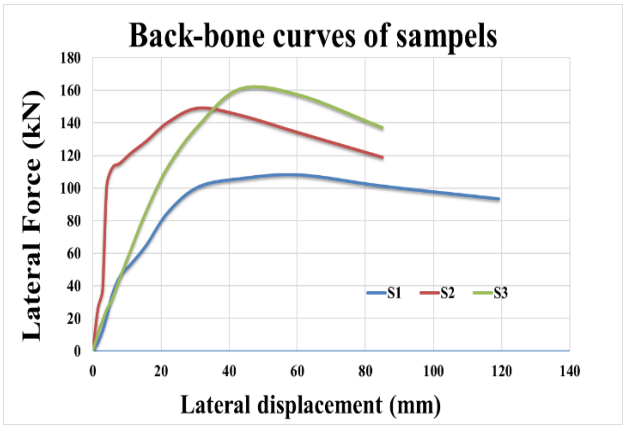

Fig. 5: Hysteresis and back-bone of samples (blue line is for S1-red line is for S2-green line is for S3)

3.Finite Element Modeling

To check more closely and get more information about the behavior between the frame and light concrete, the laboratory samples were modeled using ABAQUS software. Abaqus, a powerful finite element analysis (FEA) software, offers advanced capabilities for simulating the complex behavior of masonry walls. The modeling process can be approached in two primary ways: micro modeling, which captures the detailed interactions between individual bricks and mortar, and macro modeling, which simplifies the wall into a single unit for faster analysis.

The purpose of this modeling is to validate numerical and laboratory models. In the next stages of research to find a comprehensive behavior of moment frame models, we need to ensure that our modeling has high reliability and accuracy. For modeling in ABAQUS software, we need information from the model, which we obtained the required information according to the tests performed in the materials section. For modeling, we need information such as the compressive strength of DLFC materials and moment frame concrete, yielding and breaking characteristics of reinforcements, which were obtained in the study of these cases. One of the most important modeling parameters is how to model the mortar between the DLFC blocks. For this purpose, according to the mortar shear strength test obtained from the direct cutting test, the adhesion equal to 0.63 Mpa and the friction angle value equal to 23 degrees were calculated. These characteristics were modeled as interaction between blocks.

In semi-brittle materials, damage can be introduced by evaluating the fracture energy lost to create cracks. In the CDP (Concrete Damage Plasticity) model, the damage in concrete is expressed by two scalar terms dt which is tensile damage and dc which is compressive damage. In these two cases, the damage is defined by reducing the elastic stiffness after loading. In Abaqus software, we first select the desired compressive stress-strain curve. Different behavioral models are presented in cyclic and uniform loading. In modeling, we used cyclic behavior.

In this behavioral model, the amount of inelastic stress-strain is calculated first, then the inelastic strain is calculated with the step-by-step $\varepsilon_c^{in} = \varepsilon_c - \frac{\sigma_c}{E_0}$ formula. The behavioral model of tensile mode is also defined based on the failure defined in Figure 5. In this way, inelastic strain is defined according to the $\varepsilon_t^{ck} = \varepsilon_t - \frac{\sigma_t}{E_0}$ relationship. How to apply damage to pressure and tension according to laboratory results is defined as below its failure limit.

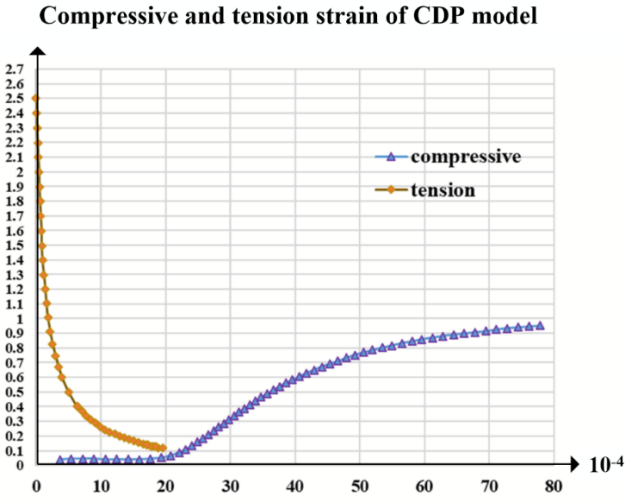

Fig. 6: The behavioral model of tensile mode compressive and tension strain

The model was modeled according to the size and arrangement of rebars in the software. The elements used for the concrete are of the cube type with 8 nodes and the elements used for the reinforced concrete used in the intermediate frame are of the 4-node type. The results obtained from the modeling of the samples are shown according to Figure 6 in the steps of maximum displacement and maximum drift.

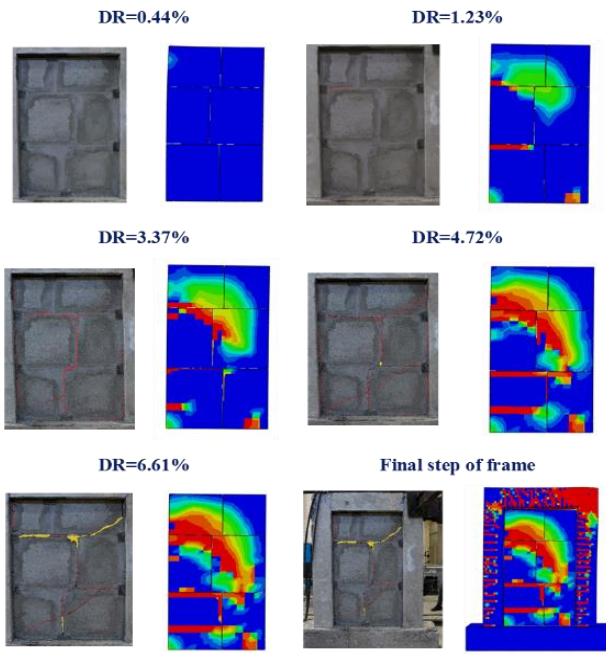

(a)

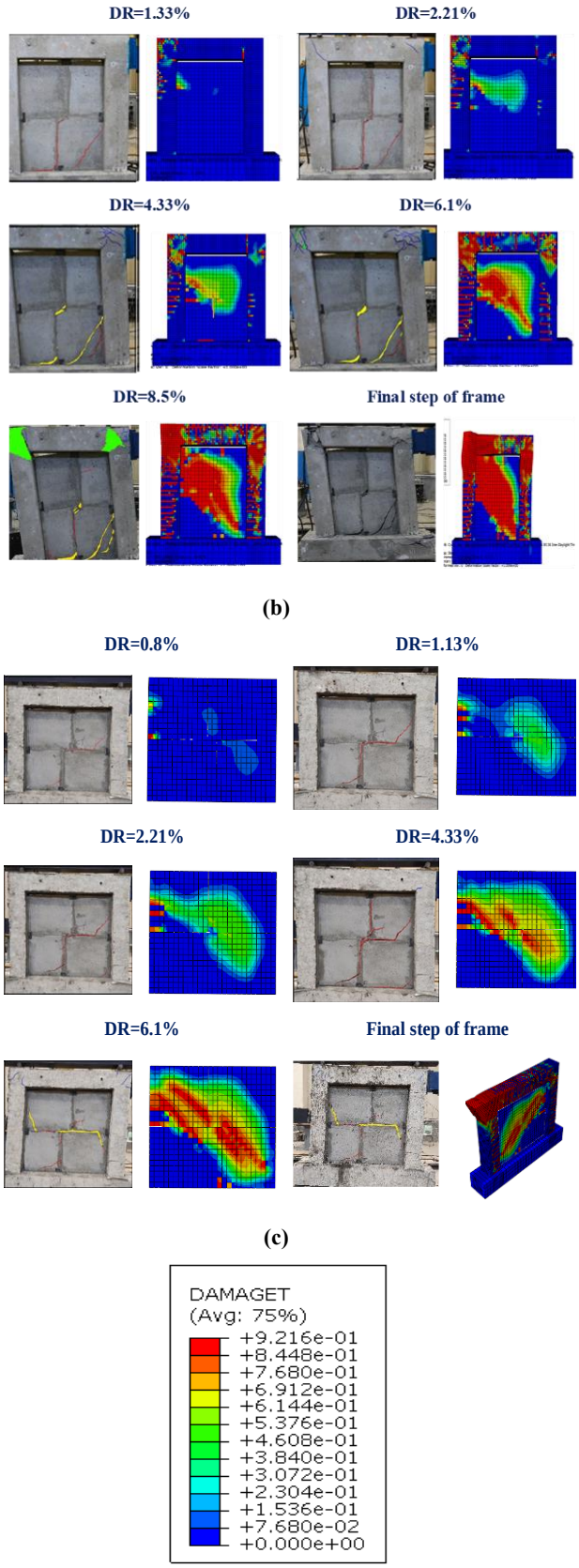

Fig. 7: Step-by-step drift and principal stress (a) Sample S1, (b) Sample S2 and (c) Sample S3

As can be seen from the results of the analysis, the cracking of the panels is very similar to the cracks created in the test. The most common type of failure of DLFC concrete blocks is diagonal failure. This indicates that the blocks participate in bearing the lateral force as diagonal members. Another type of block failure is sliding between them. In the middle part, this failure is more than the other parts. And this means that in the middle part, in addition to the pressure, sliding is also a determining factor.

3.1 Bare frame and equivalent strut modeling

In order to compare the infill frame with DLFC materials with the bare frame, bare frame modeled in opensees software. In Figure 8 complete modeling information is shown. The nonlinear behavior of the beam and columns of the concrete RC frame was used using the extended plasticity method with fiberization of the sections, and by introducing a certain number of integration points and concrete and steel materials, the global deformation of the frame was determined. The materials used in the concrete bending frame, which include steel and concrete, were selected according to the Opensees library.

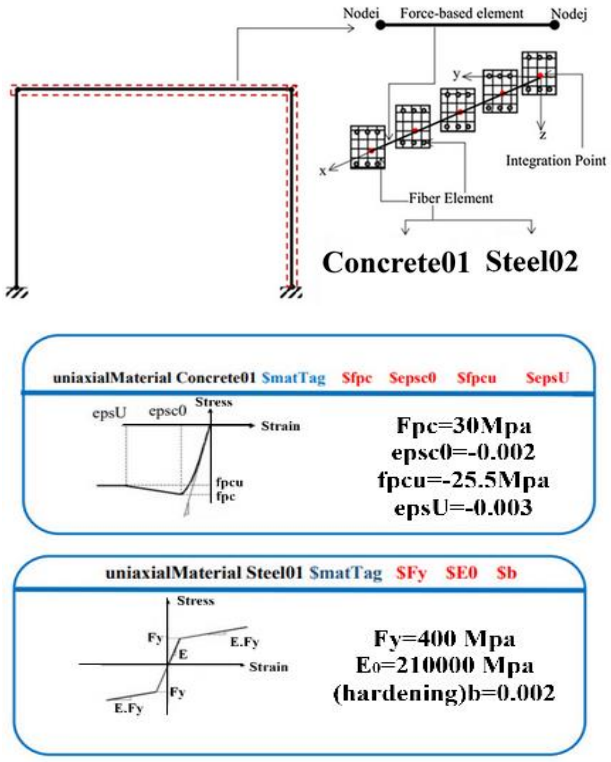

Fig. 8: Parameters of the Opensees model

In the modeling of fiber sections, we considered the number of divisions along the length and width of the section to be 15 and the number of integration points along the length of the element to be 8. The confinement coefficient of the concrete core was considered to be 1.48.

According to the failure results of DLFC blocks, because the behavior and failure of concrete materials are more diagonal, then the materials inside the frame can be modeled as an equivalent strut. One of the best methods for modeling infill-walls is the method presented in the FEMA 356 [34] instruction, where the width of the equivalent handle is obtained according to the relationships 1 and 2. The Figure 9 shows how to model the equivalent strut.

$$w=0.175(\lambda \cdot h\mathrm{col})^{-0.4} \cdot r\mathrm{inf} \quad (1)$$

$$\lambda_h = \sqrt[4]{\frac{E_m.t.\sin 2\theta}{4.E_c.I_c.h_m}} \quad (2)$$

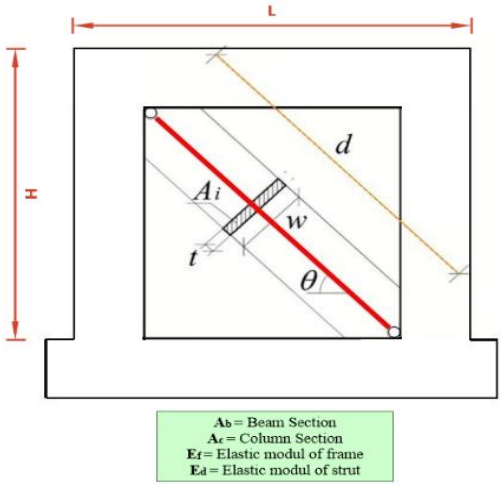

Fig. 9: Equivalent strut

4. Benchmark Structures

To investigate the behavior of RC frames systems with light concrete intermediate frames, SAC models were studied as examples. These structures meet the design considerations of the regulations that are located in the areas of Los Angeles, California, Seattle, and Boston, USA, and are based on the participation of three non-profit organizations, SEAOC, CUREE, and ATC. The plan, views of the floors, and the details of the sections of these three bending frames are shown in Figure 10.

The frames are the same. The use of these records is beneficial as they cover a diverse range of earthquake magnitudes, distances, and site conditions. This variety facilitates a more comprehensive evaluation of structural behavior when subjected to different seismic loads. By incorporating FEMA records, researchers can anchor their time history analyses in trustworthy and widely recognized data, thereby bolstering the reliability of their findings and ensuring alignment with established seismic design codes.

Therefore, to check the accuracy of the obtained results, a frame resistant to bending in the north-south direction was considered in each building. Due to the existing symmetry, each frame can bear half of the gravity load and lateral forces. The amount of gravity load in these structures was applied as Gravity column. The 9-story SAC model building has a basement and the first floor is one of the soft floors. This building has a soft floor and to ignore this issue, this building was modeled as a foothold at the ground level. Also, in the 9-story model, to eliminate the effect of the form floor, the height of the first floor was slightly reduced.

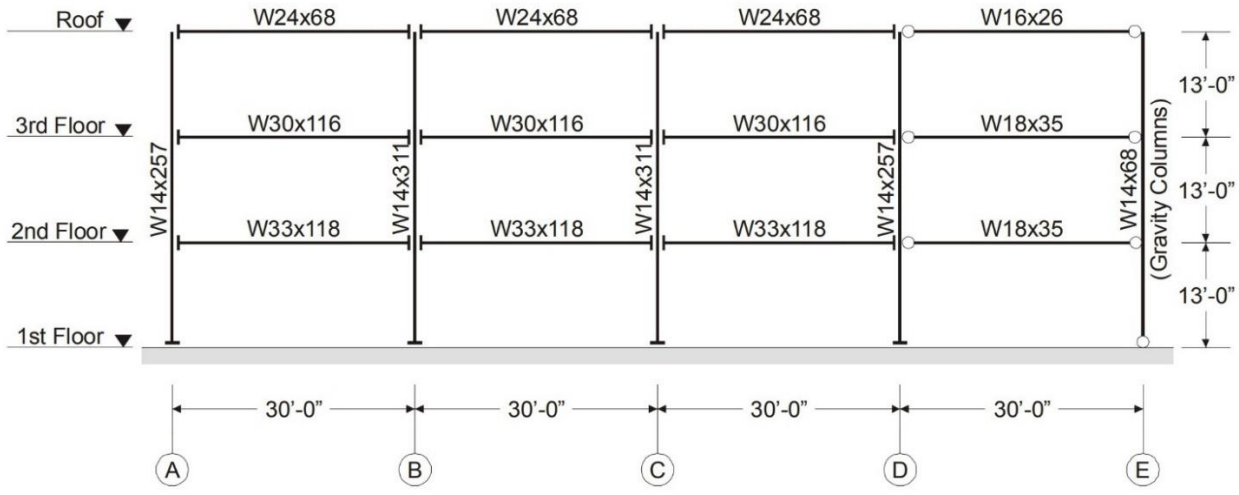

(a)

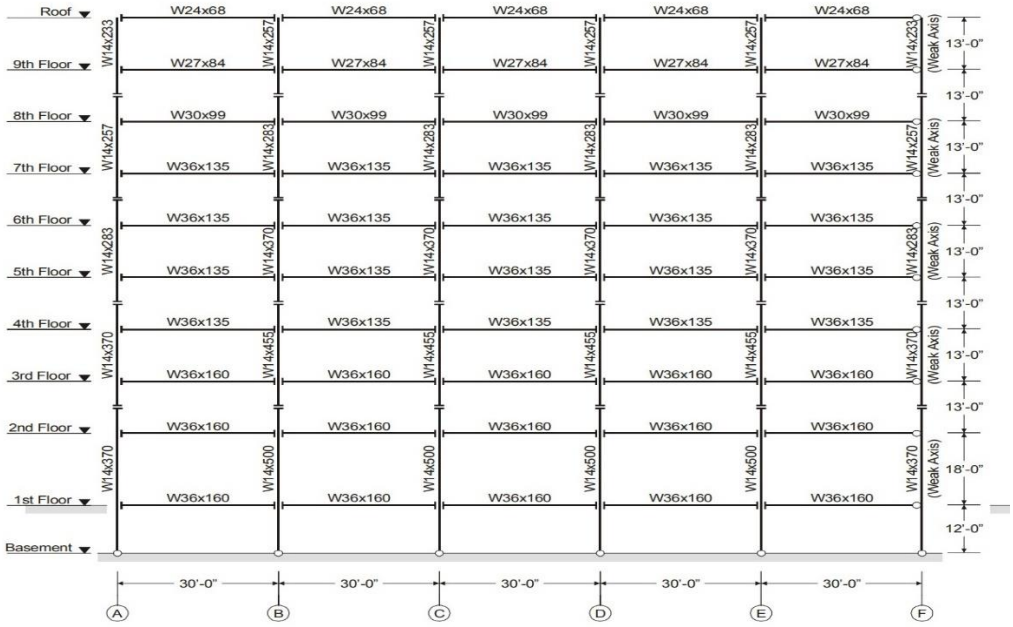

(b)

Fig. 10: SAC models (a) 3-story and (b) 9-story details of profiles and dimensions

4.1 Record for NTHA

The used accelerometers were collected based on table (C-2) of FEMA-440 and all of them are from type C soil. The important point in choosing the accelerometers is that they are all of the type of normal earthquakes and none of them are near to the fault and the directivity effect is not seen in it. In this study, it has been tried to use 15 acceleration to show the results It is worth mentioning that the method proposed in FEMA-440 was used to scale this group of acceleration maps, which were extracted from the peer site. The use of these records is beneficial as they cover a diverse range of earthquake magnitudes, distances, and site conditions. This variety facilitates a more comprehensive evaluation of structural behavior when subjected to different seismic loads. By incorporating FEMA records, researchers can anchor their time history analyses in trustworthy and widely recognized data [39], thereby bolstering the reliability of their findings and ensuring alignment with established seismic design codes. The design spectrum used for the design of 3 and 9-story structures is according to Figure 11. The other characteristic of records has been showed in Table 1.

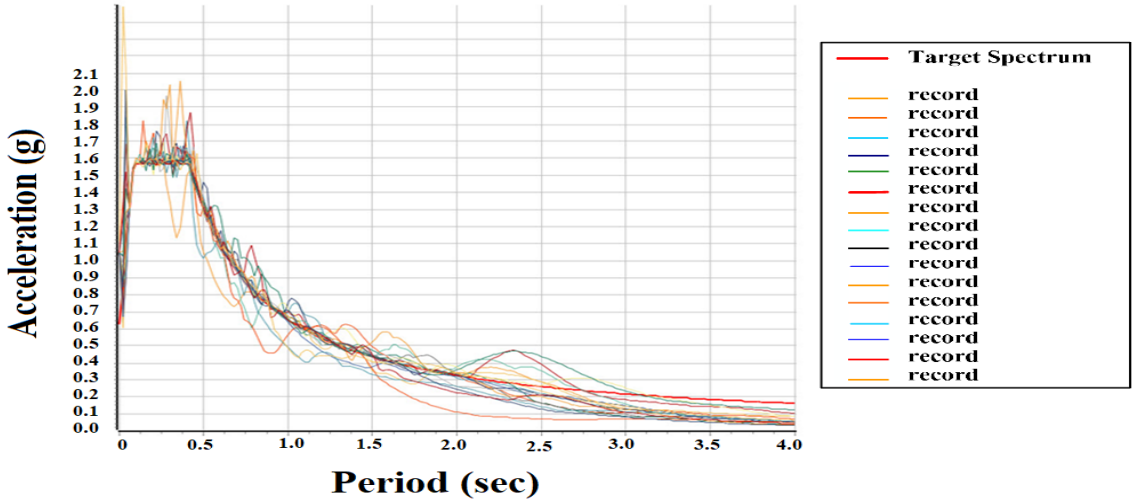

Fig. 11: acceleration for NTHA

Table 1: Scaled and unscaled records for NTHA of SAC buildings

Number	Date	Earthquake Name	Magnitude (Ms)	Station Name	Station Number	Unscaled PGA	Scaled PGA
R1	10/15/1979	Imperial Valley	6.8	El Centro, Parachute Test Facility	5051	0.2g	1.04912
R2	10/17/1989	Loma Prieta	7.1	Anderson Dam, Downstream	1652	0.239g	0.6566g
R3	10/17/1989	Loma Prieta	7.1	APEEL 7, Pulgas	58378	0.153g	0.63371g
R4	10/17/1989	Loma Prieta	7.1	Fremont, Mission San Jose	57064	0.121g	0.91834g
R5	10/17/1989	Loma Prieta	7.1	Gilroy #6, San Ysidro Microwave site	57383	.167g	0.72161g
R6	10/17/1989	Loma Prieta	7.1	Gilroy, Gavilon College Phys Sch Bldg	47006	0.349g	0.59422g
R7	10/17/1989	Loma Prieta	7.1	Monterey, City Hall	47377	0.071g	0.59761g
R8	10/17/1989	Loma Prieta	7.1	San Francisco, Dimond Height	58130	0.11g	0.78839g
R9	10/17/1989	Loma Prieta	7.1	Saratoga, Aloha Ave	58065	.495g	0.92382g
R10	10/17/1989	Loma Prieta	7.1	Yerba Buena Island	58163	0.066g	0.90531g
R11	6/28/1992	Landers	7.5	Yermo, Fire Station	12149	0.167g	0.73324g
R12	4/24/1984	Morgan Hill	6.1	Gilroy #6, San Ysidro	57383	0.28g	0.66746g
R13	4/24/1984	Morgan Hill	6.1	Gilroy, Gavilon College Phys Sci	47006	0.095g	0.66366g
R14	1/17/1994	Northridge	6.8	Castaic, Old Ridge Route	24278	0.504g	0.76358g
R15	1/17/1994	Northridge	6.8	Lake Hughes #1, Fire station#78	24271	0.085g	1.03645g
R16	1/17/1994	Northridge	6.8	Littlerock, Brainard Canyon	23595	0.07g	0.83458g
R17	7/8/1986	Palmsprings	6	Fun Valley	5069	0.129g	1.02662g
R18	2/9/1971	San Fernando	6.5	Pasadena, CIT Athenaeum	80053	0.107g	0.88103g
R19	2/9/1971	San Fernando	6.5	Pearblossom Pump	269	0.133g	1.11152g

Now, to scale the records used or pay attention to the design range presented above, we use the method of matching records. The algorithm presented by Al Atik and Abrahamson [35] was proposed and the scaling of records was done by Seismomatch software [36].

4.2 Results of NTHA

The results of the time history analysis are shown in Figure 12, comparing the roof displacement history in both bare frame and infill frame with DLFC (use of equivalent strut).

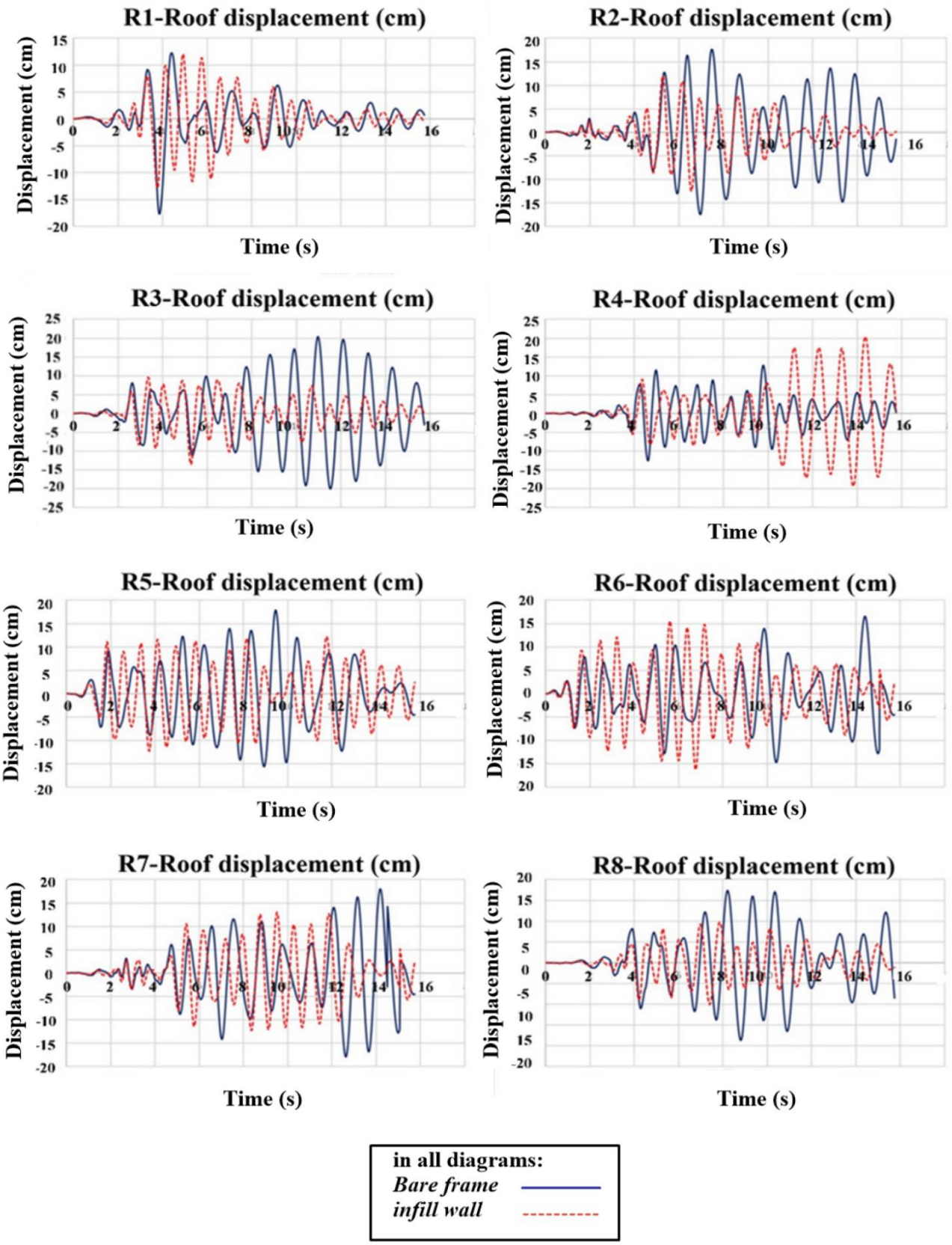
R1-Roof displacement (cm)
R2-Roof displacement (cm)
R3-Roof displacement (cm)
R4-Roof displacement (cm)
R5-Roof displacement (cm)
R6-Roof displacement (cm)
R7-Roof displacement (cm)
R8-Roof displacement (cm)
Displacement (cm)
Time (s)
in all diagrams:
Bare frame
infill wall

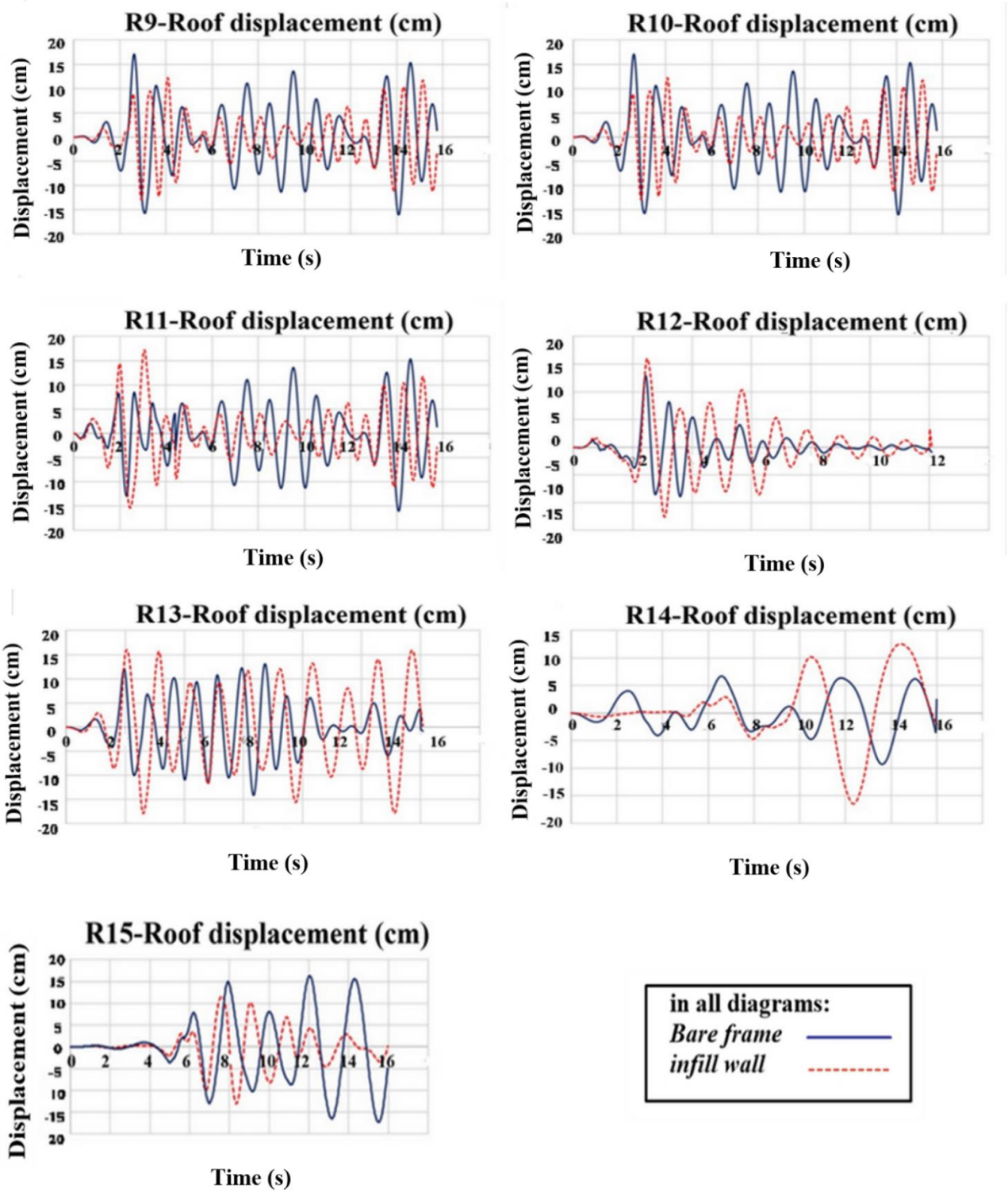
R9-Roof displacement (cm)
R10-Roof displacement (cm)
R11-Roof displacement (cm)
R12-Roof displacement (cm)
R13-Roof displacement (cm)
R14-Roof displacement (cm)
R15-Roof displacement (cm)
Displacement (cm)
Time (s)
in all diagrams:
Bare frame
infill wall

(a)

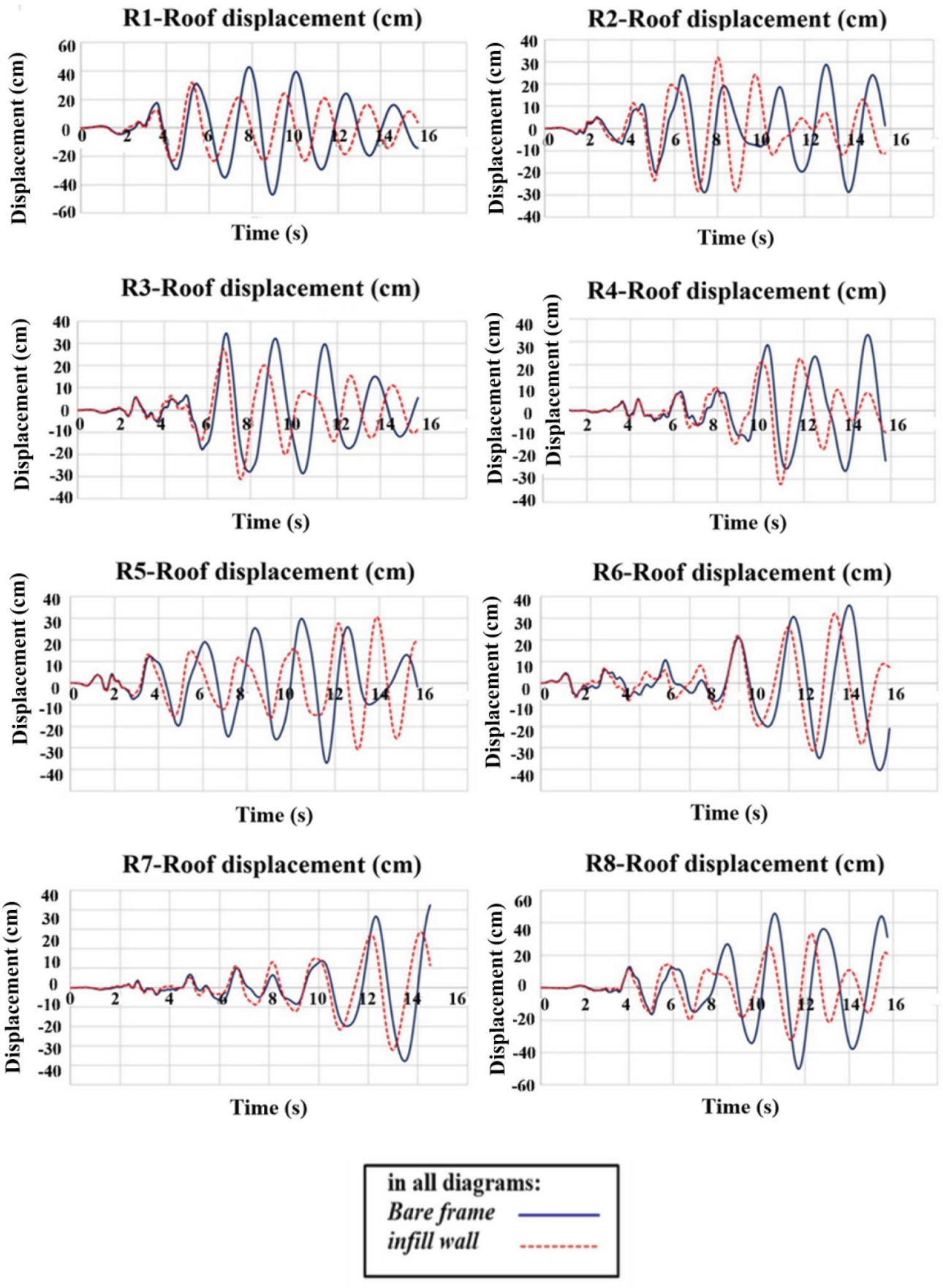
R1-Roof displacement (cm)
R2-Roof displacement (cm)
R3-Roof displacement (cm)
R4-Roof displacement (cm)
R5-Roof displacement (cm)
R6-Roof displacement (cm)
R7-Roof displacement (cm)
R8-Roof displacement (cm)
Displacement (cm)
Time (s)
in all diagrams:
Bare frame
infill wall

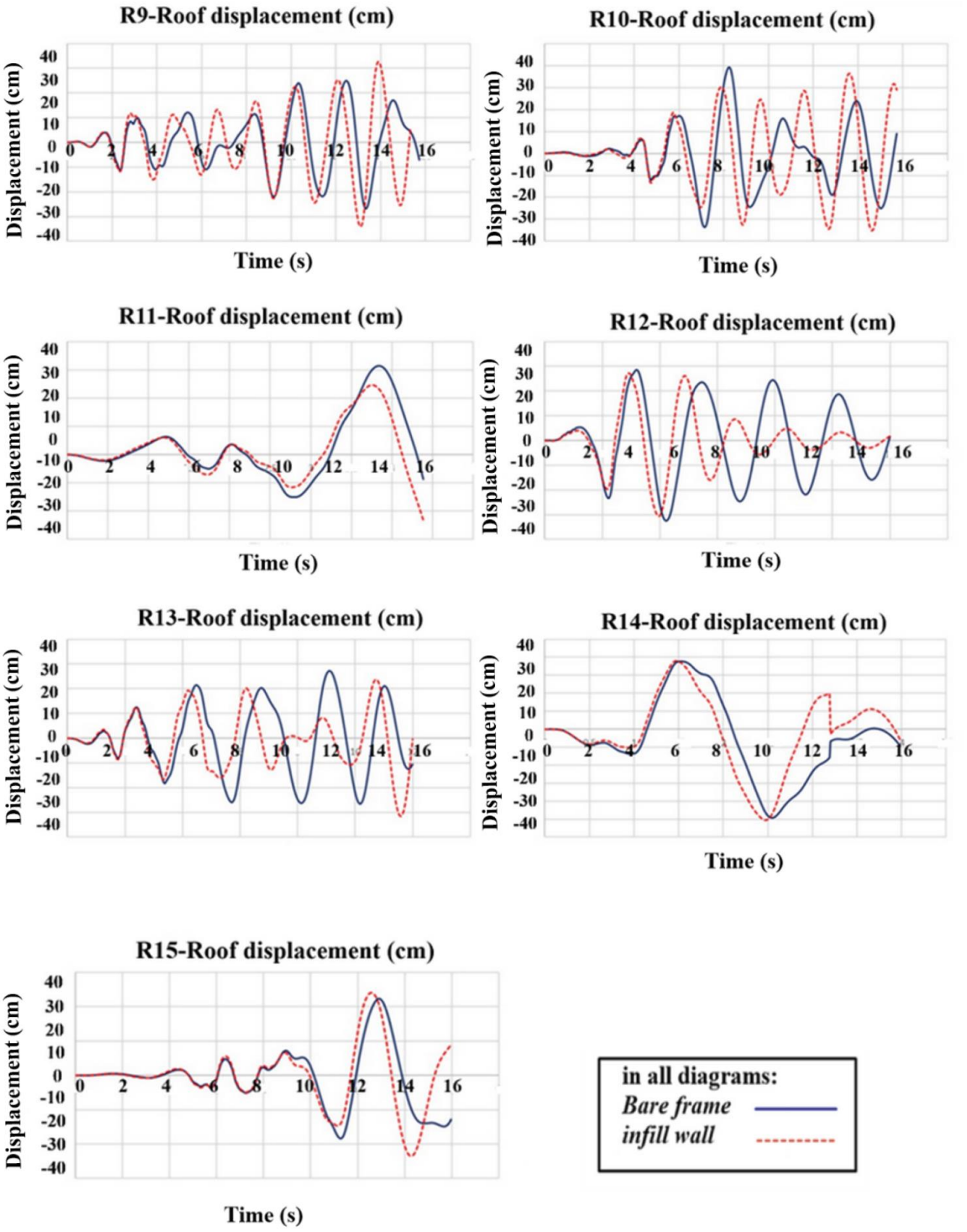

(b)

Fig. 12: Comparing the roof displacement of bare and infill frame (a) Response of 3-stories (b) Response of 9-stories

According to the results obtained in the time history analysis, the amount of the displacements obtained in the 3-story structure in the case where the frame is bare is more than the case where there is an infill frame. Of course, in some analyses, such as records 9, 10 and 2, the displacements are more or equal to the frame state with the moment frame, and the reason for this can be the change in the periodicity of the system and the frequency content of the earthquake. In the case of the 9-story structure, the displacement of the frame with the moment frame is less than the case of the empty frame in all cases, and it shows that the impact of the infill frame was better in this structure. In general, if we take a general look at the responses of the system with the infill frame, it shows that the addition of the light concrete infill frame studied in this research does not only increase the displacement of the structure, but also reduces the displacement.

5. Cost analysis

A key aspect of comparing infill walls is the discussion of costs in full-scale construction projects. In this section, we examine the expenses associated with three commonly used infill materials cement blocks, clay blocks, and bricks and compare them to the DLFC materials [38] investigated in this study. This analysis provides valuable insights into the economic implications of selecting different infill options in building construction. The parameters selected for the price comparison encompass several key factors: material costs, equipment costs, material waste, and workmanship expenses. Given that the costs of materials and construction practices can differ significantly across countries, a standardized base price was utilized for this comparison. This approach ensures a more equitable evaluation of the various infill wall options.

We established the cost of the brick wall as the baseline price, referred to as (A). Based on this reference point, we calculated the prices of other materials. The labor cost for two workers was estimated under the assumption of an 8-hour workday. For consistency, the wall thickness was set at 20 cm, focusing solely on the infill area. This depth was uniformly applied across all materials considered. A detailed comparison of these costs is presented in Table 2. The findings of this analysis indicate that while the cost of DLFC which comprises ultrafine filler, pumice, polystyrene, polypropylene, and polyvinyl alcohol is higher compared to other materials, the overall expense remains comparable. This is attributed to the quicker installation process and reduced material wastage associated with DLFC. Consequently, the advantages in efficiency help offset the initial cost increase.

Table 2: Cost comparison between DLFC materials and 3 common traditional infill wall materials with depth of 20cm according to the base cost of (A)

		Material cost	Equipment cost	Waste of materials (%)	Final cost per square meter	Workmanship costs 8 hours of work in one day (2 persons)	The area that is built every hour
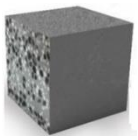	**DLFC block**	2.57A	1.067A	0	3.64A	8.89A	12
	**Bricks**	1.7A	0.89A	5%	2.756A	8.89A	5
	**Cement block**	A	0.89A	5%	1.9389A	8.89A	3.75
	**Clay block**	1.11A	0.89A	5%	2.056A	8.89A	2.5

6. Conclusion

1. The finite element results show very well the cracks created in the samples, which shows the correct way of numerical modeling. As shown in the different drifts, the amount of crack propagation in successive test steps is very similar to the finite element results
2. Experiments show that the closer the ratio of the height of the blocks to their width is, the diagonal cracks are closer to 45 degrees. Although increasing the height of the sample increased the degree of cracks.
3. Most of the failures in the samples are diagonal, according to this point, blocks can be modeled with a strut.
4. Modeling of mortar between blocks using adhesion and friction coefficient shows the accurate behavior between blocks in finite analysis modeling.
5. SAC building models were modeled in Opensees software for accuracy measurement. Infilled frame were modeled as compressive equivalent struts. The width and area of the struts were modeled according to FEMA criteria, and the results showed a decrease in the response of the structures with the presence of the infill frame.
6. The results of the time history analysis show a decrease in the displacement of the roof of the samples, which is one of the desirable effects of the presence of DLFC blocks.
7. The amount of period shift of structures with DLFC blocks is very low, which reduces the dangerous effects of earthquakes due to the change in the frequency content of earthquakes.
8. Finally, structures with DLFC blocks can be examined due to their low weight, which is a very effective factor in structures. Because they are more malleable compared to walls with lighter-weight building materials.

References

[1] Messaoudi, A., et al., Influence of Masonry Infill Wall Position and Openings in the Seismic Response of Reinforced Concrete Frames. Applied Sciences, 2022. 12(19): p. 9477.

[2] Mucedero, G., D. Perrone, and R. Monteiro, Epistemic uncertainty in poorly detailed existing frames accounting for masonry infill variability and RC shear failure. Earthquake Engineering & Structural Dynamics, 2022. 51(15): p. 3755-3778.

[3] Xu, Q., et al., Numerical simulation study of progressive collapse of reinforced concrete frames with masonry infill walls under blast loading. Modelling and Simulation in Engineering, 2022. 2022.

[4] Abdel-Hafez, L.M., A. Abouelezz, and F.F. Elzefeary, Behavior of masonry strengthened infilled reinforced concrete frames under in-plane load. HBRC Journal, 2015. 11(2): p. 213-223.

[5] Zhang, C., et al., Seismic behavior of novel low-damage precast infill walls with sliding joints for reinforced concrete frame. Earthquake Engineering & Structural Dynamics, 2022. 51(15): p. 3730-3754.

[6] De Risi, M.T., et al., In-plane behaviour and damage assessment of masonry infills with hollow clay bricks in RC frames. Engineering Structures, 2018. 168: p. 257-275.

[7] Feng, D.-C., et al., Investigation of 3D effects on dynamic progressive collapse resistance of RC structures considering slabs and infill walls. Journal of Building Engineering, 2022. 54: p. 104421.

[8] Murty, C. and S.K. Jain. Beneficial influence of masonry infill walls on seismic performance of RC frame buildings. in 12th world conference on earthquake engineering. 2000.

[9] Wararuksajja, W., et al., Seismic design method for preventing column shear failure in reinforced concrete frames with infill walls. Journal of Building Engineering, 2021. 44: p. 102963.

[10] Petrović, M., N. Mojsilović, and B. Stojadinović, Masonry walls with a multi-layer bed joint subjected to in-plane cyclic loading: An experimental investigation. Engineering Structures, 2017. 143: p. 189-203.

[11] O'Brien, P., et al., Measures of the seismic vulnerability of reinforced concrete buildings in Haiti. Earthquake Spectra, 2011. 27(1_suppl1): p. 373-386.

[12] Ahiwale, D.D., D.-P.N. Kontoni, and P.L. Darekar, Seismic performance assessment of reinforced concrete frames with different bracing systems. Innovative Infrastructure Solutions, 2023. 8(3): p. 102.

[13] Gentile, R., et al., Non-linear analysis of RC masonry-infilled frames using the SLaMA method: part 1—mechanical interpretation of the infill/frame interaction and formulation of the procedure. Bulletin of Earthquake Engineering, 2019. 17: p. 3283-3304.

[14] Dhir, P.K., et al., A macro-model for describing the in-plane seismic response of masonry-infilled frames with sliding/flexible joints. Earthquake Engineering & Structural Dynamics, 2022. 51(12): p. 3022-3044.

[15] Panto, B., et al., Macro-modelling approach for assessment of out-of-plane behavior of brick masonry infill walls. Engineering Structures, 2019. 181: p. 529-549.

[16] Roosta, S. and Y. Liu, Development of a Macro-Model for concrete masonry infilled frames. Engineering Structures, 2022. 257: p. 114075.

[17] Furtado, A., et al. Cost-effective analysis of textile-reinforced mortar solutions used to reduce masonry infill walls collapse probability under seismic loads. in Structures. 2020. Elsevier.

[18] Rosnitschek, T., et al., Correlations of geometry and infill degree of extrusion additively manufactured 316l stainless steel components. Materials, 2021. 14(18): p. 5173.

[19] Paulay, T. and M.N. Priestley, Seismic design of reinforced concrete and masonry buildings. Vol. 768. 1992: Wiley New York.

[20] Yon, B., Seismic vulnerability assessment of RC buildings according to the 2007 and 2018 Turkish seismic codes. Earthquakes and Structures, 2020. 18(6): p. 709-718.

[21] Committee, M.S.J., Building Code Requirements and Specification for Masonry Structures: Containing Building Code Requirements for Masonry Structures (TMS 402-08/ACI 530-08/ASCE 5-08), Specification for Masonry Structures (TMS 602-08/ACI 530.1-08/ASCE 6-08) and Companion Commentaries. 2008: Masonry Society.

[22] Altın, S., et al., Strengthening masonry infill walls with reinforced plaster. Proceedings of the Institution of Civil Engineers-Structures and Buildings, 2010. 163(5): p. 331-342.

[23] Dehghani, A., F. Nateghi-Alahi, and G. Fischer, Engineered cementitious composites for strengthening masonry infilled reinforced concrete frames. Engineering Structures, 2015. 105: p. 197-208.

[24] Facconi, L. and F. Minelli, Retrofitting RC infills by a glass fiber mesh reinforced overlay and steel dowels: Experimental and numerical study. Construction and Building Materials, 2020. 231: p. 117133.

[25] Koutas, L., S. Bousias, and T. Triantafillou, Seismic strengthening of masonry-infilled RC frames with TRM: Experimental study. Journal of Composites for Construction, 2015. 19(2): p. 04014048.

[26] Akhoundi, F., et al., In-plane behavior of cavity masonry infills and strengthening with textile reinforced mortar. Engineering Structures, 2018. 156: p. 145-160.

[27] Aksoylu, C. and R. Sezer, Investigation of precast new diagonal concrete panels in strengthened the infilled reinforced concrete frames. KSCE Journal of Civil Engineering, 2018. 22: p. 236-246.

[28] Preti, M., N. Bettini, and G. Plizzari, Infill walls with sliding joints to limit infill-frame seismic interaction: large-scale experimental test. Journal of Earthquake Engineering, 2012. 16(1): p. 125-141.

[29] Erdem, I., et al., An experimental study on two different strengthening techniques for RC frames. Engineering Structures, 2006. 28(13): p. 1843-1851.

[30] Shirzadi, T. and F. Ahmadi Danesh Ashtiani, Mechanical behavior of new lightweight concrete with fiber and ingredients. Numerical Methods in Civil Engineering, 2023.

[31] Movahhed AS, Shirkhani A, Zardari S, Mashayekhi M, Farsangi EN, Majdi A. Modified endurance time method for seismic performance assessment of base-isolated structures. Journal of Building Engineering. 2023 May 15;67:105955..

[32] Tiam shirzadi, F. Ahmadi Danesh Ashtiani, Ehsan Noroozinejad Farsangi,A novel Ductile Lightweight Fiber-Reinforced Concrete (DLFC)

[33] infill for seismic-prone zones: Experimental and numerical investigations, Structures, Volume 63,2024,

[34] F. FEMA, "461," Interim testing protocols for determining the seismic performance characteristics of structural and nonstructural components, report no. FEMA-461. Federal Emergency Management Agency Washington, DC, 2007

[35] F. 356, "FEMA 356 Prestandard," ed: US Federal Emergency Management Agency Washington, DC, USA, 2000.

[36] L. A. Atik, N. Abrahamson, J. J .Bommer, F. Scherbaum, F. Cotton, and N. Kuehn, "The variability of ground-motion prediction models and its components," Seismological Research Letters, vol. 81, no. 5, pp. 794-801, 2010.

[37] N. Abrahamson, "Program SeismoMatch v2," Software capable of adjusting earthquake accelerograms to match a specific design response spectrum, using the wavelets algorithm proposed by Abrahamson [1992] and Hancock et al.[2006], 2006.

[38] Shirzadi, T., Ahmadi Danesh Ashtiani, F. Mechanical behavior of new lightweight concrete with fiber and ingredients. Numerical Methods in Civil Engineering, 2024; 8(3): 22-28. doi:10.61186/NMCE.2023.781

[39] Sadeghi-Movahhed A, Billah AM, Shirkhani A, Mashayekhi M, Majdi A. Vulnerability assessment of tall isolated steel building under variable earthquake hazard levels using endurance time method. Journal of Structural Integrity and Maintenance. 2024 Jan 2;9(1):2314816.